ORIGINAL PAPER

ATLID, ESA atmospheric backscatter LIDAR for the ESA EarthCARE mission

João Pereira do Carmo[1] · Geraud de Villele[2] · Arnaud Helière[1] · Kotska Wallace[1] · Alain Lefebvre[1] · François Chassat[2]

Abstract

The ATmospheric LIDAR (Light Detection and Ranging), ATLID, is part of the payload of the Earth Cloud, Aerosol and Radiation Explorer (EarthCARE) mission, the sixth Earth Explorer Mission of the European Space Agency (ESA) Living Planet Programme (http://esamultimedia.esa.int/docs/SP_1279_1_EarthCARE.pdf). The EarthCARE payload consists of four instruments that will, in a synergetic manner, retrieve vertical profiles of clouds and aerosols, and the characteristics of the radiative and micro-physical properties, to determine flux gradients within the atmosphere and top of atmosphere radiance and flux. ATLID's task is to provide vertical profiles of optically thin cloud and aerosol layers, as well as the altitude of cloud boundaries. With that purpose ATLID emits < 35 ns duration laser pulses with 40 mJ energy in the UV, at a repetition rate of 51 Hz, while pointing in a near nadir direction along track of the satellite trajectory. The backscatter signal is collected by a 620 mm aperture telescope and is then filtered and redirected through the optics of the instrument focal plane assembly, in such a way that the atmospheric Mie and Rayleigh scattering contributions are separated and independently measured. After the manufacturing, qualification and delivery of all ATLID units, the optical and electrical integration has been conducted in parallel to assemble the Optical Flight Model (OFM) and the Electrical Flight Model (EFM). These two models, precursor to the instrument integration, allowed the early execution of the first performance and functional tests. Following these initial verification activities, and with the latest integration of the flight laser cooling system, the instrument assembly approaches its final flight configuration, paving the way for the ambient performance and environmental test campaigns at full instrument level.

Keywords Lidar · Aerosol · Clouds · UV laser

1 Introduction

1.1 The EarthCARE mission

EarthCARE [1, 2] is a joint collaborative mission conducted between ESA and the Japan Aerospace Exploration Agency (JAXA) that delivers the Cloud Profiling Radar (CPR) instrument. The EarthCARE mission basic objective is to improve the understanding of the cloud-aerosol-radiation interactions and Earth radiative balance, so that they can be modelled with better reliability in climate and in numerical weather prediction models. Specifically, EarthCARE scientific objectives are:

- Observation of the vertical profiles of natural and anthropogenic aerosols on a global scale, their radiative properties and interaction with clouds;
- Observation of the vertical distributions of atmospheric liquid water and ice on a global scale, their transport by clouds and their radiative impact;
- Observation of cloud distribution ('cloud overlap'), cloud precipitation interactions and the characteristics of vertical motions within clouds;
- Retrieval of profiles of atmospheric radiative heating and cooling through the combination of the retrieved aerosol and cloud properties.

✉ João Pereira do Carmo
joao.pereira.do.carmo@esa.int

1 European Space Agency - ESTEC, Noordwijk, The Netherlands

2 Airbus Defence and Space, Toulouse, France

To provide atmospheric observations globally, Earth-CARE will be placed in a Sun-Synchronous Orbit with a repeat cycle of 25 days. A low operational altitude of 393 km has been selected to enhance the performance of the two active instruments. The quasi-polar orbit will allow to cover all latitudes from equator to $\pm 83°$.

The Mean Local Solar Time of 14:00 resulted from Phase A observation needs trade-off. It is close to the start of convection, which is initiated mainly in the early afternoon over land, whereas near-noon is the most representative of diurnal average for Top Of Atmosphere (TOA) broadband reflected Short Wave flux and relative errors in SW flux retrieval are smallest when SW signal is high; sun-glint and coherence with A-train satellite orbits were also taken into consideration. The satellite is designed for an in-orbit lifetime of three years and will carry sufficient consumables for a possible one-year extension of mission. The operational availability has been specified as 95% for the routine phase.

The spacecraft configuration results from extensive trade-offs performed during the early phases of the Project. Optimization took place according to the major mission requirements, in particular the accommodation of the four instruments payload, their fields of view, and the impacts of the relatively low orbit required to enhance the active instruments' performance. The streamlined shape of the spacecraft, with its trailing solar array, as seen on Fig. 1, minimizes its cross-section and reduces the residual atmospheric drag.

1.2 The EarthCARE payload

To fulfil its objectives, the EarthCARE payload comprises four instruments [3, 4], a High Spectral Resolution UV ATmospheric LIDar (ATLID), a Cloud Profiling Radar (CPR) [5] with Doppler capability, a Multi-Spectral Imager (MSI) and a Broad-Band Radiometer (BBR) [6].

An important aspect of the mission is the required co-registration of the multi-instrument payload data. The instrument viewing geometry, as seen in Fig. 2, illustrates the satellite ground track, the CPR beam at normal nadir, the lidar beam de-pointed backward by 3° to reduce specular conditions, the across track swath of the MSI with its offset in the anti-sun direction to mitigate sun-glint and finally the 3 BBR views in nadir, forward and backward directions required to retrieve the emitted flux.

The task of ATLID [7] is to provide vertical profiles of optically thin cloud and aerosol layers, as well as the altitude of cloud boundaries. The measurements of ATLID are close to the nadir direction. The instrument emits short laser pulses at a repetition rate of 51 Hz along the horizontal track of the satellite trajectory, so that several shots can be locally averaged to improve the signal to noise ratio. As presented in Fig. 3, ATLID profile measurements have a vertical resolution of about 100 m from ground to an altitude of 20 km and 500 m from 20 km to 40 km altitude.

The CPR, developed by JAXA, is a high power 94 GHz Doppler radar that measures the vertical profiles of clouds along the sub-satellite track. It emits microwave pulses at variable repeat frequency that penetrate deep into lower cloud layers, which are not visible to optical instruments. The lowest measurement altitude extends to -1 km, to permit the use of surface backscatter, and the highest measurement altitude is around 20 km. Vertical sampling interval is 100 m.

The MSI will observe at nadir with a spatial resolution of about 500 m with an across-track swath of 150 km that is offset across track to minimize sun-glint. The instrument is composed of two push-broom type imaging cameras, a Thermal Infrared camera (TIR) and a Visible-Near infrared, Short wave infrared camera (VNS) and will provide images in seven spectral channels.
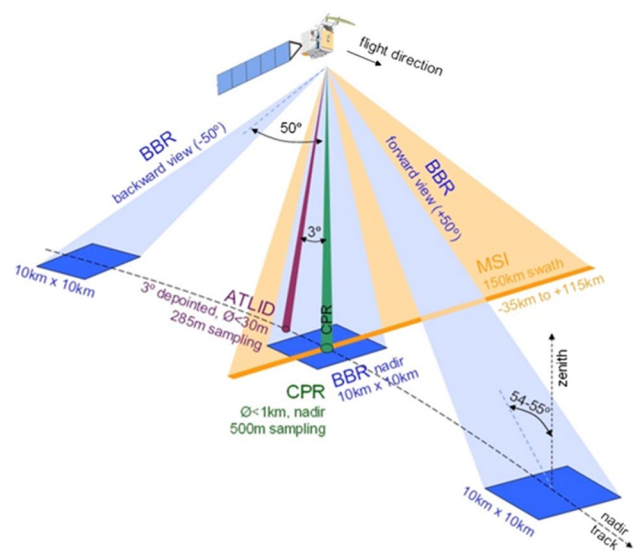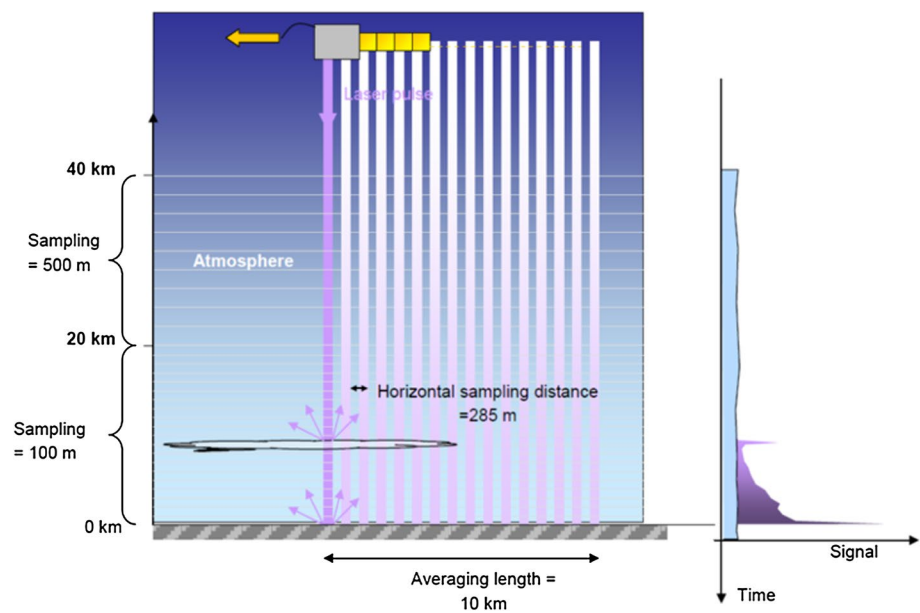

Fig. 1 Artist's view of the EarthCARE satellite in-orbit

Fig. 2 EarthCARE instruments viewing geometry

Fig. 3 ATLID resolution and sampling specifications

The BBR provides an estimate of the reflected (short wavelength range < 4 μm) and emitted (long wavelength range 4 to > 50 μm) fluxes at the top of the atmosphere for a 10 km square scene (nadir). The instrument will measure the top of atmosphere (TOA) radiance, at the same location, in two wavebands, using three along track views that point nadir, forward and aft of nadir. BBR performs measurements in a Total Wave (TW) and a Short Wave (SW) band. Long Wave (LW) data is estimated by subtraction of SW from TW channel measurements.

The four instruments will provide [8], in a synergetic manner, information on cloud and aerosol vertical structure of the atmosphere along the satellite track, as well as information about the horizontal structures of clouds and radiant flux from sub-satellite cells.

2 The atlid instrument

2.1 ATLID principle

ATLID [9] is a high spectral Resolution LIDAR operating in the ultra-violet domain (355 nm) that uses the fact that interaction of light with molecules and aerosols leads to different spectra scattering effects. Whereas the Brownian motion of molecules induces a wide broadening of the incident light spectrum, the scattering with an aerosol does not affect the spectral shape of the incident light. As a consequence, a simple means of separating the backscattering contributions consists of filtering the backscattered spectrum with a high spectral resolution filter centred on the emitted wavelength. In this way, the instrument is able to separate the relative contribution of aerosol (Mie) and molecular (Rayleigh)

scattering, which allows the retrieval of the aerosol optical depth. Co-polarised and cross-polarised components of the Mie scattering contribution are also separated and measured on dedicated channels. The operating wavelength in the UV spectral range was selected as the molecular scattering is high enough to measure more accurately extinction profiles and aerosols/thin clouds thickness and because laser technology (Nd:YAG laser with frequency tripling conversion) is available for operation in this spectral region; eye safety versus field of view was also a consideration.

2.2 ATLID design and sub-units

ATLID, being assembled and tested by Airbus Space and Defence in Toulouse, is designed as a self-standing instrument (with its own instrument control unit), thereby reducing the mechanical coupling of instrument/platform interfaces and allowing better flexibility in the satellite integration sequence. The instrument is based on a bi-static architecture consisting of two independent main sections, the emitter chain and the receiver chain, see Fig. 4. This architecture was preferred to monostatic architecture (emission and reception paths share the same telescope) as it allows efficient mitigation of Laser Induced Contamination risk, by avoiding cross-contamination of emission and reception chain, by permitting the full pressurization of the emission path, and by limiting the number of optical surfaces exposed to vacuum.

The instrument mechanical support is shared between a Stable Structure Assembly (SSA) and the Housing Structure Assembly (HSA). The SSA contains the telescope, equipped with the focal plane optics, and the optical emission chain, as presented in Fig. 4. The HSA is supporting the electronic
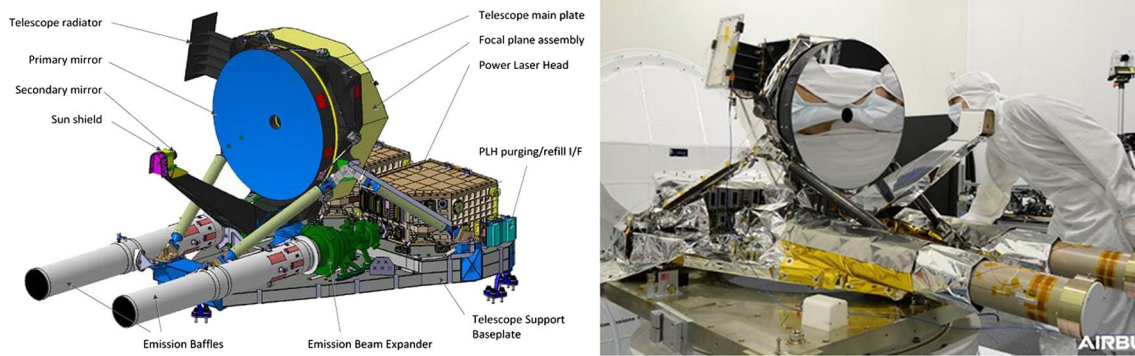
Fig. 4 Stable structure assembly (SSA) of ATLID with both emission and receiver chains

units and their radiator, the detection chain and the harness. Stability performance of this high stability assembly is favoured by the assembly of laser and optics on a single CFRP sandwich base-plate, from which all units out of the stability chain are excluded. This CFRP sandwich allows optimizing both high stiffness, for supporting both 37 kg laser units, and low hygro-thermal expansion for stability.

On the emitter chain the Transmitter Assembly (TxA), designed and manufactured by LEONARDO, is the laser source for the ATLID LIDAR. It comprises a Power Laser Head (PLH), seen in Fig. 5, seeded via a fibre optic by a Reference Laser Head (RLH), and its associated Transmitter Laser Electronics (TLE). There are two fully redundant transmitters (in cold redundancy), each including both laser heads (PLH and RLH) and electronics (TLE). The PLH design is based on a diode-pumped tripled Nd:Yag laser, providing a high energy pulse at 355 nm. In the nominal measurement mode, it is operated in steady-state mode with 51 Hz pulse repetition frequency (PRF). While the laser transmitter is largely inheriting from the Aladin instrument development for the AEOLUS mission [10], significant evolution has been achieved by the fact that the ATLID PLH is sealed and pressurized to improve its

tolerance to Laser Induced Contamination. In addition, since ATLID design is based on a bi-static architecture, a Beam Steering Mirror (BSM), placed at the end of the PLH optical train, allows the control of the laser beam output direction as part of the ATLID alignment control loop system. The two laser transmitter flight models have been delivered and the first transmitter proto-flight model (PFM) has included a long burn-in test at the end of its qualification campaign, to demonstrate the successful accumulation of more than 150 MShots. Both models demonstrated compliance with the main requirements: pulse energy > 38 mJ, pulse duration < 35 ns, output beam size approx. 8×9 mm^2 and laser beam divergence < 300 µrad.

At the output of the PLH, the Emission Beam Expander (EBEX) is used to enlarge the laser beam to meet the divergence requirement and to minimize the laser fluence on the last dioptre exposed to vacuum. The EBEX is sealed and pressurized for mitigating Laser Induced Contamination. The EBEX is followed by a dedicated and long emission baffle that aims to protect the EBEX output window from external contamination during instrument and satellite assembly, test and flight.
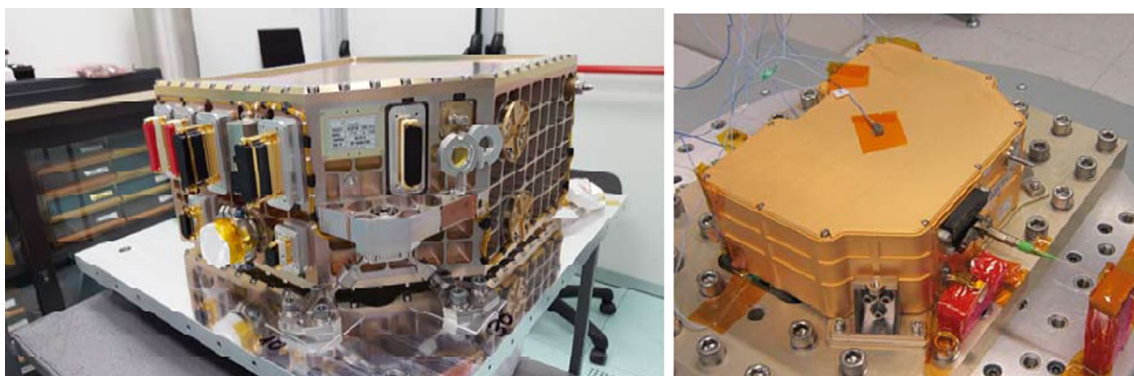
Fig. 5 Power laser head (Leonardo) and reference laser head (TESAT) flight models

The receiver telescope is an afocal Cassegrain, with 620 mm primary mirror diameter, which collects the backscattered light. It is made of Silicon Carbide to ensure high stability. Several units are then part of the receiver optics train, going from telescope output to detector fibres' entrance. The optics chain is comprised of the entrance filter optics (narrow interference filter with less than 1 nm bandwidth), the blocking filtering optics (spatial filtering with a field-stop delimiting the 65 µrad field-of-view) and one Fabry–Perot etalon (used for high spectral resolution filtering). The signal is transported to the detectors by means of fibre couplers, allowing deporting the whole detection chain onto the anti-sun wall for passive cooling. Part of the flux is split off at the focal plane assembly entrance and imaged onto the Co-Alignment Sensor (CAS), which provides laser spot position information and is a key unit of the ATLID co-alignment control loop subsystem.

At the heart of the receiver chain the High Spectral Resolution Etalon (HSRE), Fig. 6, developed by RUAG Space System, differentiates and filters the Mie and Rayleigh components of the backscatter signal, routing these (including splitting co-polarized from cross polarized light) towards the relevant detection channels. The key performance requirement of the HSRE is achieving the UV high transmittance on Mie co-polarized channel with a Full-Width-Half-Maximum (FHWM) of 0.3 pm. The unit concept is based on a Fabry–Perot (FP) etalon used in combination with polarisation beam-splitters (PBS) and quarter-wave plates. The Fabry–Perot etalon acts as a filter, transmitting only the narrow Mie signal and reflecting the wider Rayleigh signal.

With this filtering design implementation, special care needs to be taken for the spectral and polarisation cross talk corrections. For this reason, all the relative calibration parameters are subjected to a comprehensive on ground calibration and can also be calibrated in-flight in nominal instrument mode, hence without interrupting the nominal measurements. The cross-talk parameters allow to convert the instrument signals, coming from the three instrument channels, into three signals that are directly proportional to the pure backscatter products (Rayleigh, Mie copolar and Mie cross polar). The instrument raw data needs to be corrected mainly for spectral cross talk, but a contribution for polarisation cross talk also exists. The spectral cross talk is calibrated on ground by scanning a dedicated source across the receiver frequency range. In addition, this calibration is improved in flight on a routine basis by continuously processing the stratospheric backscatter (for Mie co-polar cross-talk) and cloud or ground echoes (for the Rayleigh cross-talk). This approach allows to minimize systematic errors (such as instrumental parameter drifts), because the spectral cross-talk correction parameters can be updated continuously, as there is no need for measurement interruption. The spectral cross-talk in the Rayleigh channel shall be known to better than 20% of its value, while for the Mie co-polar channel this is improved to be better than 10%.

The polarisation cross talk parameters are mainly calibrated on ground. Two Polarisation Beam Splitters (PBS) are implemented on each Mie channel and the Rayleigh beam passes one PBS in double pass. While measurements at HSRE unit level shown polarisation cross talk values of < 0.2% for all channels, these values are expected to increase when all the optics of the receiver chain are fully integrated. For this reason, the polarisation transmission measurements are to be repeated several times during the full instrument development and qualification campaigns, to provide accurate data for the final calibration on ground. The polarisation cross-talk in the Mie co-polar and cross-polar channels shall be known to better than 10% of its value. Additionally, in flight calibration measurements, such as making use of high altitude backscatter Rayleigh signals (for Mie cross polar calibration), are also to be considered to correct any possible long-term drift effects.

To lock the TxA laser wavelength with the HSRE, a spectral calibration of the laser is to be performed once a month in flight to compensate for laser frequency drifts and other detuning contributors. The frequency calibration approach that is retained for ATLID consists of a laser frequency scan around etalon central frequency. The atmospheric echo is
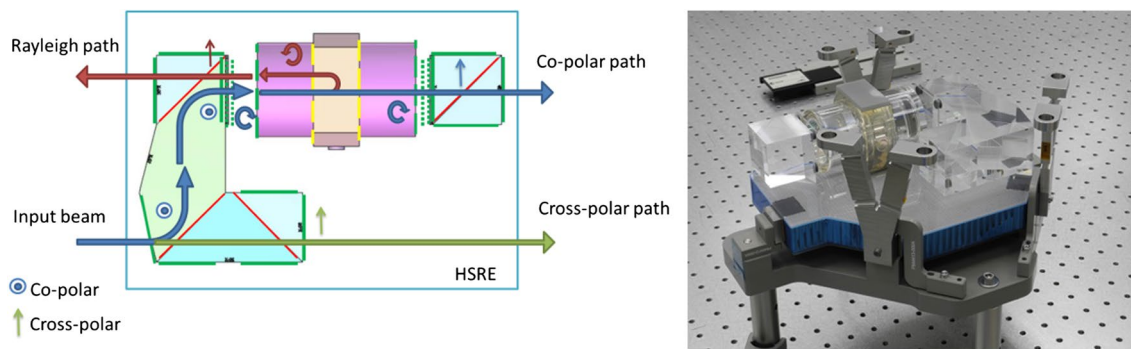

Fig. 6 HSRE functional scheme and HSRE unit (RUAG)

acquired with the same operation sequence as nominal measurement, while 41 frequency steps are implemented for the Fine Spectral Calibration (FSC) operation. During the FSC, the laser frequency is scanned from -500 to $+500$ MHz, relative to the nominal laser frequency, with steps of 25 MHz. This laser frequency calibration measurement sequence duration is typically 10 min.

The science channels detection functions are ensured by the Memory CCD and the Instrument Detection Electronics (IDE). The detection chain shall be able to measure near single photon events to meet the worst case radiometric performance requirements. The selected design provides high response together with an extremely low noise, thanks to on-chip storage of the echo samples, which allows delayed read-out at very low pixel frequency (typically below 50 kHz). Combined with an innovative read-out stage and sampling technique, the detection chain provides an extremely low read-out noise (approximately 2e- rms per sample).

The transmitter and receiver co-alignment is achieved thanks to the cooperative function of the BSM (beam steering at transmitter side) with the CAS (imaging beam subsystem at receiver side). It aims at maintaining a very good co-alignment between emission line-of-sight and reception line-of-sight, which is of prime importance to guarantee an optimum geometrical coupling and a good spectral matching. The co-alignment control loop allows correcting for SSA thermo-elastic deformation expected in orbit, biases due to launch and thermo-elastic settling and any mid-term drifts. The control loop includes:

- The Co-Alignment Sensor (CAS), stable with respect to receiver line of sight;
- The Instrument Detection Electronics (IDE), which receive the images from the CAS at 51 Hz and performs averaging over 32 shots, to improve signal to noise ratio and reduce data rate towards the control and data management unit;
- The control and data management unit, ACDM (ATLID Control and Data Management Unit), that receives the averaged images from the IDE, performs background subtraction, applies the centroiding algorithm to obtain the spot centre position and calculates the command to be realized by the mechanism to centre the spot in the sensor CCD matrix;
- The Beam Steering Mechanism (BSM), part of the transmitter assembly, receives the command from the controller and steers the laser emission path accordingly.

The BSM has its own control loop (BSM drive electronics) to reach the desired position of the mirrors on the emission path. The co-alignment performance specification is ± 4 μrad peak, current expected performance being below ± 3 μrad.

The control and data management ACDM unit, including software designed to provide full autonomy in operation management, ensures the synchronization between laser emission and backscatter signal acquisition, the data processing and data stretching toward the spacecraft, the thermal regulation functions, the co-alignment control loop software (including co-alignment sensor images processing and centroiding algorithms) as well as the beam steering mechanism commanding, the TM/TC and observability management.

2.3 Proto-flight model development

ATLID instrument development is based on a proto-flight model (PFM) approach: critical sub-systems such as laser transmitter, beam expander, beam steering mechanism and detector front-end have been subject of specific efforts in terms of early breadboards, electrical models or qualification models to minimize the risks [11].

The ATLID instrument development logic and models' definition was tailored to allow an efficient development with early validations of the main design drivers to minimize risks. An initial Electrical Engineering Model (EEM), built around representative electronics units, allowed verifying ATLID internal electrical interfaces and software functions, detection chain susceptibility to EMC, and co-alignment control loop function. Detection Flight Models have been assembled in parallel and used for early verification activities of detection performance.

Following the successful ATLID instrument CDR, completed in 2015, all the PFM units have been delivered to Airbus for instrument integration. The instrument integration is now near completion and the instrument performance and qualification campaign started second quarter 2019, followed by the instrument delivery to the satellite prime by the end of 2019.

3 Atlid development plan: OFM and EFM

3.1 Optical and electrical parallel programs

To anticipate at maximum the instrument verification while the integration is not complete, ATLID PFM verification program was divided into two subprograms: The Optical Flight Model (OFM) and the Electrical Flight Model (EFM). As can be seen in Fig. 7, both OFM and EFM programs were integrated and tested in parallel at Airbus Defence and Space Toulouse cleanrooms.

The Optical Flight Model (OFM), including the receiver telescope and focal plane assembly installed on the SSA, was used to validate the structural stability of the receiver assembly and for characterization of the optical receiver
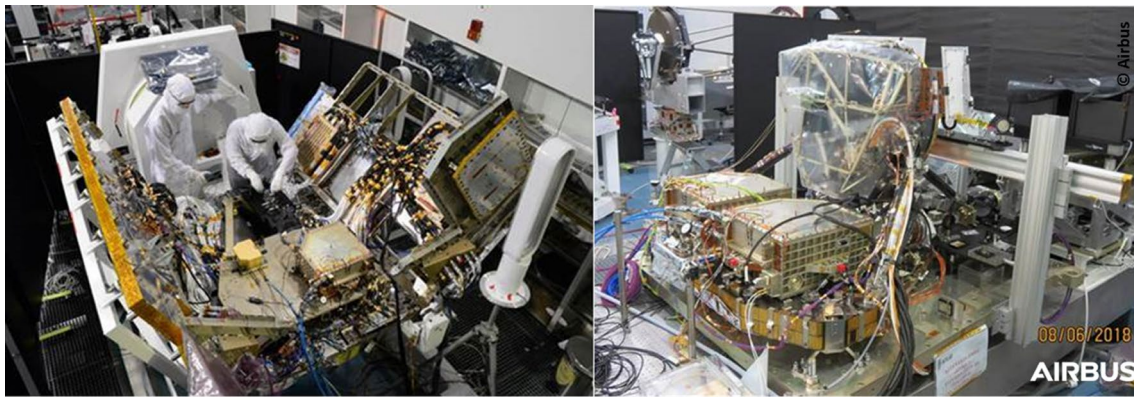
Fig. 7 ATLID EFM model on the left, and ATLID OFM model on the right

chain performance. The Electrical Flight Model (EFM), including the HSA with the flight model electronics and harness, was used to establish and verify the electrical coupling between the different units and perform the first part of the instrument functional tests.

3.2 OFM mechanical testing description and results

The OFM mechanical test, Fig. 8, consisted of applying the spacecraft environments to the systems or subsystems to confirm optical stability as well as mechanical strength over the expected lifetime. The objective of mechanical testing was to de-risk in advance the most critical parts on ATLID receiver chain side:

- M1/M2 (primary/secondary) mirrors, as well as the main plate (focal plane assembly support), are composed of Silicon Carbide, offering high thermal stability with a great mechanical strength;
- Structural adhesive joints reach their maximum limits during mechanical vibration tests. The computations and

simulations of bonded parts in dynamic environments are key elements derived from modelling and test activities heritage;
- Optical contacting inside the HSRE consists of molecular adhesion. Its stability under acoustic loads was beforehand checked by vibration tests and computations.

During the vibration qualification tests accelerometers attached to the item under test are used to control the shaker. The choice of these accelerometers and the ability to predict their responses (with regards to stress levels on SiC parts, adhesive and optical contacting) more particularly remain the most important tasks of the test.

One criticality for this kind of mechanical test, beyond overstress risks, is the handling of cleanliness; an ISO 5 mobile cleanroom hood was used to ensure a controlled environment, also a dedicated protection during acoustic tests.

The OFM passed with success vibration and acoustic loads applied in the 3 axis configurations, thus confirming OFM mechanical strength, as well as optical stability, for
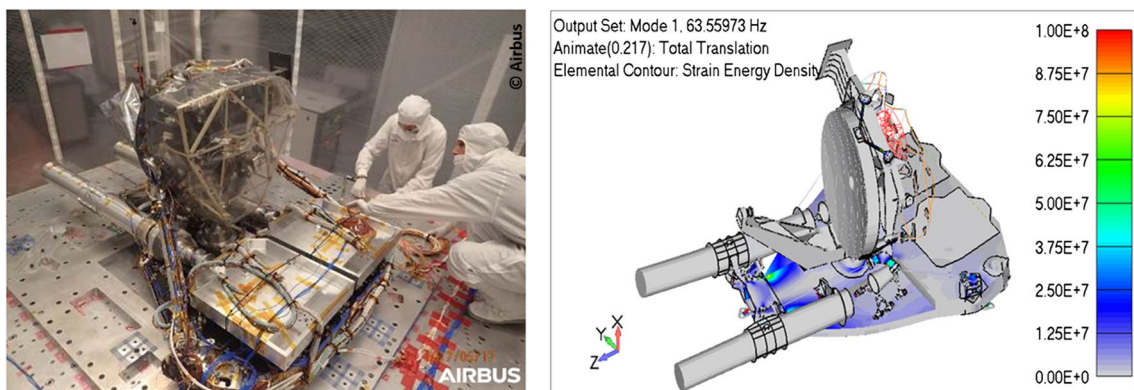

Fig. 8 ATLID OFM in Y axis vibration test configuration on shaker at Intespace Toulouse (left)/ATLID OFM FEM Y principal mode @ 63.6 Hz (right)

the specified launch environment. In particular, the superposition of the low level curves, as well as the global/fundamental signals of the qualification runs, indicates that the structure integrity is maintained after launch simulation. Moreover, the optical stability was confirmed to remain within specification by the means of theodolite measurements consistent to better than 100 μrad. In addition, a strong correlation between the finite element model and the test results has been observed in terms of frequency (<6%). Finally, these results permitted to adjust the finite element model in the frame of the preparation of ATLID mechanical test at instrument PFM level.

With the implementation of a bi-static architecture design and the use of a dedicated co-alignment control loop system, the thermo-elastic deformation impact is limited and no instrument structural and thermal model has been tested. The direct integration and testing of a proto-flight model remain a great challenge, in particular due to instrument complexity, while there is no direct heritage or recurrent design.

3.3 Optical tests configurations for OFM receiver

ATLID instrument OFM receiver part is composed of the telescope and the Focal Plane Assembly (FPA), where all the receiver optical filtering functions are implemented:

- Broad band background rejection and polarisation alignment with Entrance Filter Optics unit (EFO);
- Geometric Receiver Field Of View (RFOV) definition with the Blocking Filtering unit (BF);
- Co-Alignment Sensor (CAS) unit;
- High Spectral Resolution Etalon (HSRE) that splits the receiver signal onto the three channels of interest for backscattering: Mie Cross-Polarisation, Mie Co-Polar and Rayleigh;
- Fibre Coupling Assembly (FCA) injecting the signals into 3 fibres.

The optical test aims at measuring the OFM characteristics, in particular the field of view dimension, the background rejection and the receiver channel transmission. The 3 channels verification at OFM level did not include the flight detectors, which are located on ALTID external radiator and connected via optical fibres.

Due to the reduced RFOV and the high resolution filtering stage, the OGSE (Optical Ground Support Equipment) source and injection performance becomes critical to ensure proper instrument characterization; this includes the collimation control (considering instrument defocus effect of gravity or air to vacuum), the vignetting control in the reduced RFOV, the polarisation purity control, the OGSE

laser source frequency stability and adjustability, and the energy monitoring.

The obtained results are in line with ATLID radiometric budget. Spectral scanning transmissions and angular spatial scanning are as expected (Table 1 and Fig. 9). Moreover, these performances were confirmed after OFM environmental vibration tests.

3.4 OFM transmitter path alignment completion

OFM transmitter path is composed of the Power Laser Heads (PLH) and of the External Beam Expander (EBEX) and the long External Baffle tubes (EBaffle) that protect the last transmitter UV window from contamination.

PLH and EBEX models have undergone full qualification and acceptance verification respectively at Leonardo and Sodern subcontractor level. Obtained performances are a great achievement and fall within ATLID budgets (Table 2).

For integration at ATLID instrument level, the transmitter verification aimed at the alignment achievement and it has been demonstrated that the transmitters have been aligned with receiver line of sight at better than ± 70 μrad.

3.5 EFM detection program

The flight Instrument Detection Electronics (IDE) together with the Detector Fibre Assembly (DFA) have been characterized during a dedicated test at equipment level, operated by ACDM (ATLID Control and Data Management) Engineering Model. This test was performed in an Airbus Defence and Space vacuum chamber to allow nominal operation of detectors at − 30 °C, as for flight.

Operational tests on the IDE validated the detection modes such as LIDAR (nominal echo recording with variable accumulation of profile), and IMAGING for verification of fibre centring on detector. The validation was performed using a dedicated UV source with pre-determined temporal echo profile.

Detection performances have been characterized and comply with ATLID's performance needs (Table 3).

Table 1 OFM receiver characteristics measured on ground

OFM receiver characteristic	Value measured in ambient
RFOV diameter	> 60 μrad (66 μrad to be achieved in vacuum)
Wide band transmission outside interferometric filter	<0.01%
Mie-Copolar transmission max	54%
Mie-CROSS polar transmission max	60%
Rayleigh transmission max	61%
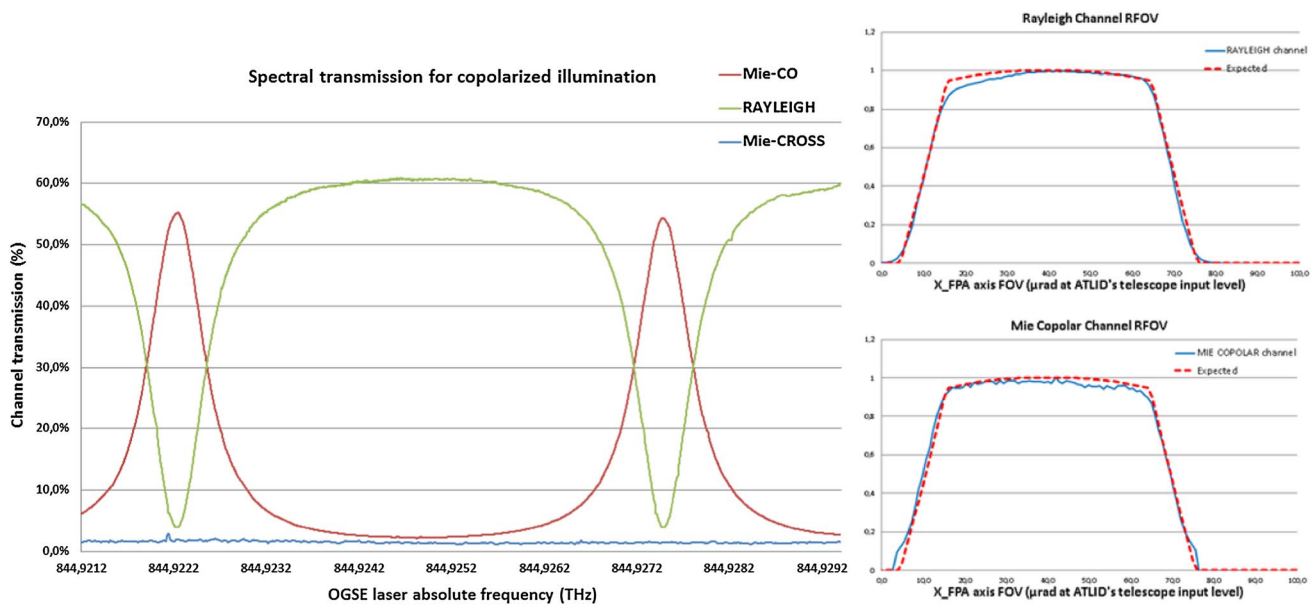
Fig. 9 OFM receiver spectral transmittance scan for co-polar illumination (left) and uniformity on angular scan on Rayleigh and Mie Co-polar RFOV channels (right)

Table 2 ATLID transmitter path characteristics at instrument exit

Characteristic	Value at ATLID exit (from PLH output measurement)
Divergence at d4sigma	28 μrad
Beam size at d4sigma	60×68 mm^2
Line of Sight compensation range	± 300μrad on both axis
Wavelength adjustability	± 12.5 GHz coarse, ± 0.5 GHz fine
Spectral width	<50 MHz @ FWHM
Wavelength stability	<3 MHz over ± 1 °C (orbital)
Max. energy	41 mJ
Pulse duration	28 ns

3.6 EFM functional testing

ATLID instrument is autonomous and requires minimum control by the satellite platform control unit; ATLID onboard software ensures all equipment telecommands and telemetries management, with general monitoring. It creates the data flow, ensures thermal control and co alignment loop control and also manages the timing synchronization.

As first step of EFM testing, the redundant path has been fully operated and submitted to systematic tests to validate operability and functionality via ACDM. Throughout 58 test procedures, all modes were tested using several thousands

Table 3 ATLID FM detection chain performance measurement results

Characteristic	ATLID EFM detection measurement
Vertical sampling	100 m samples = 22.00 Tmc (with Tmc being period of master clock = 32 MHz) 500 m samples = 106.00 Tmc WC error 0.02 Tmc = 10 cm of sample depth
Vertical crosstalk on adjacent samples	4.5% on 500 m, 19% on 100 m
Computed quantum efficiency MieCoPo/MieCross/Rayleigh	79%/75%/79%
Linearity	<$\pm$1% from 10e- to the top <$\pm$2% from 1e- to 10 e-
Dynamic margin on channels wrt predicted worst signal MieCoPo/MieCross/Rayleigh	18%/5%/12%
Noise worst case	2.2 e- rms

of automated checks, including calibration modes and Fault Detection, Isolation and Recovery (FDIR) triggering.

The laser head was operated at full power, with nominal flight operation procedures, with a set of parameters adapted for ground usage. Adjustability of PLH internal parameters, such as heating currents, nonlinear crystal temperature and pump timing, has been demonstrated and is summarized in Fig. 10. Validation of the laser operation, with instrument flight hardware, is a major successful step of functional verification.

4 Pfm final assembly and LCS integration and validation

4.1 Assembly and validation of the laser cooling system

The Laser Cooling System (LCS), presented in Fig. 11, consist of a nominal and redundant network of 2×4 diphasic mini Loop Heat Pipes, ensuring 148 W extraction from the operating laser. The PLH temperature is thus controlled at 24 °C $\pm$ 0.5 °C within one orbit, while its thermal interface is mechanically insulated from instrument housing thanks to a flexible piping, filled with ammonia, conducting the heat to an external radiator of 1.05 m^2 placed on the anti-sun side of the instrument. The design is an innovative one, having the

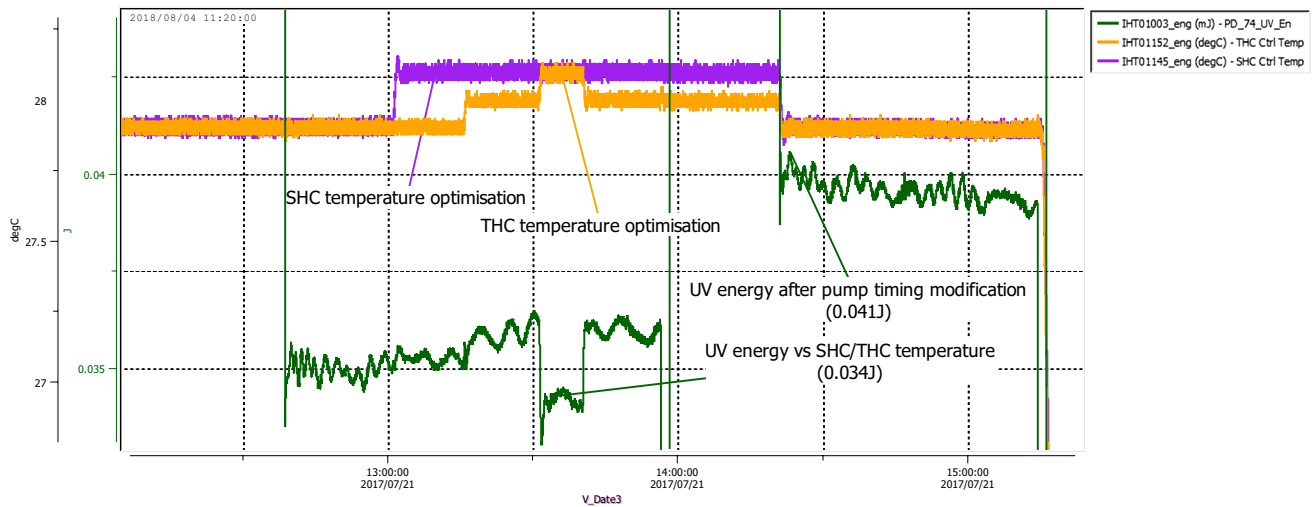**Fig. 10** Example of laser parameter control during first laser switch ON with ACDM flight unit
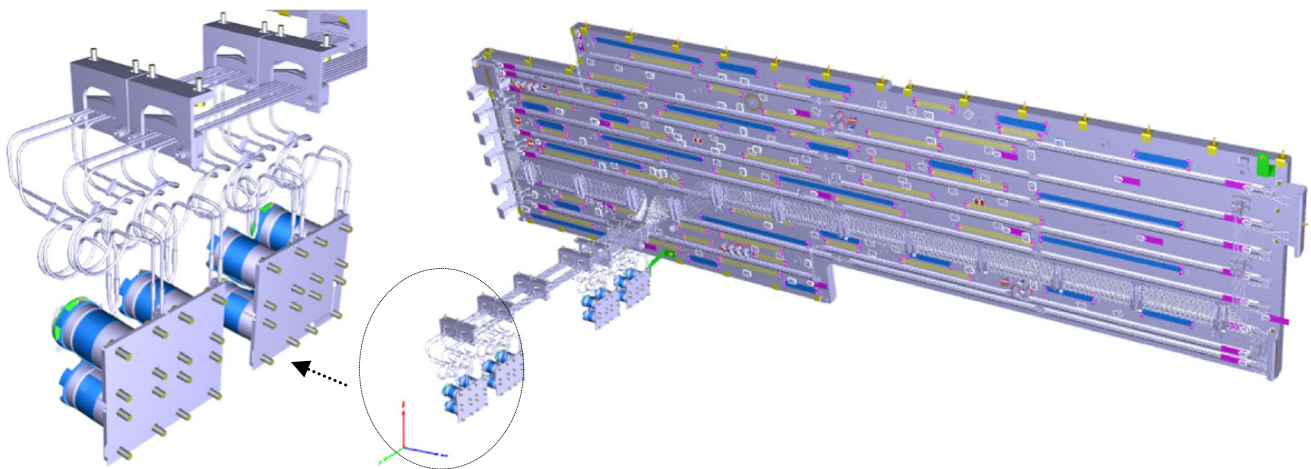

**Fig. 11** Evaporators interface to the PLHs and LCS view from its internal side

mini-LHPs operated in parallel, and the flexibility to select 4 different configuration options. The design was elaborated by Airbus in Toulouse, while the integration and the test campaign of the LCS have been done by Euro Heat Pipes (EHP) in EHP premises.

Testing of LCS thermal performance has been done at LCS level, with the LCS in 2D configuration (evaporators at the same level as the radiator) to reduce the effect of gravity and allowing to test the LCS in a representative way, close to flight performance expectations. The test validated the electrical thermal hardware, and also the safe mode of LHP inhibition system, allowing to stop excessive cooling of PLH during non-operating phases. Flight performances have been confirmed and a configuration with 6 loops operation out of 8 has been found optimum, considering PLH dissipation demands. The 2D tests also allowed to define the best start-up sequence, based on heater power distinct from PLH dissipation. After completion of the 2D phase, the LCS has been reconfigured to its final 3D shape. Thermal qualification of
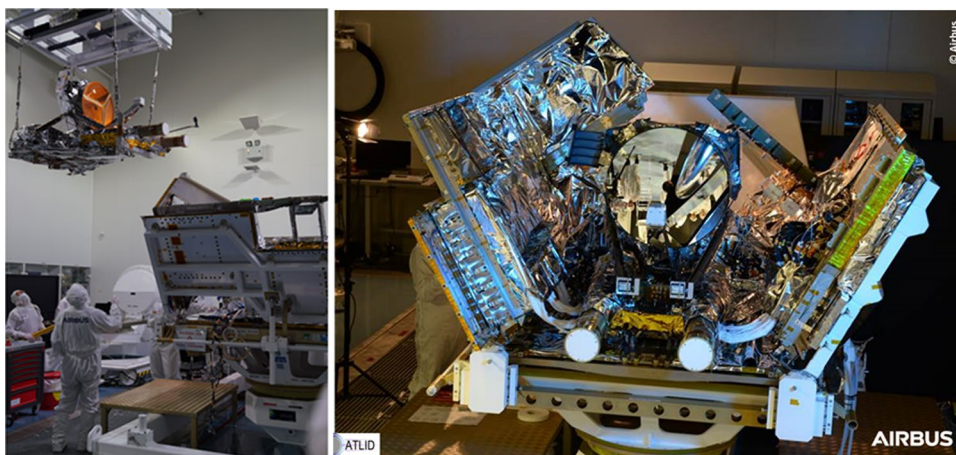
the 3D LCS was successfully completed, with vacuum non-operative thermal cycles. A dedicated Good Health Test (GHT) was implemented, to confirm each LHP ability to start-up after boost of power, and a similar test is expected to be conducted at key points of the instrument integration and testing phases. After completing the qualification campaign, the LCS was finally integrated on the correspondent HSA wall, as seen Fig. 12.

4.2 ATLID PFM final integration completion and characterization in ambient

One of the major ATLID PFM integration steps, Fig. 13, consisted of mounting of the SSA, supporting the OFM, inside of the HSA. This integration has been successfully achieved, with acceptable instrument line of sight alignment pointing error when compared with the instrument reference frame.

Following this major integration step, the LCS evaporators have been fixed against the corresponding PLH units, as seen in Fig. 14, with very careful handling to avoid any damage, especially on the tubes that transport the ammonia and which are only 2 mm in diameter.

As a last step, before closing the remaining open ATLID HSA wall, another instrument functional testing phase (now on the nominal emitter side) is performed.
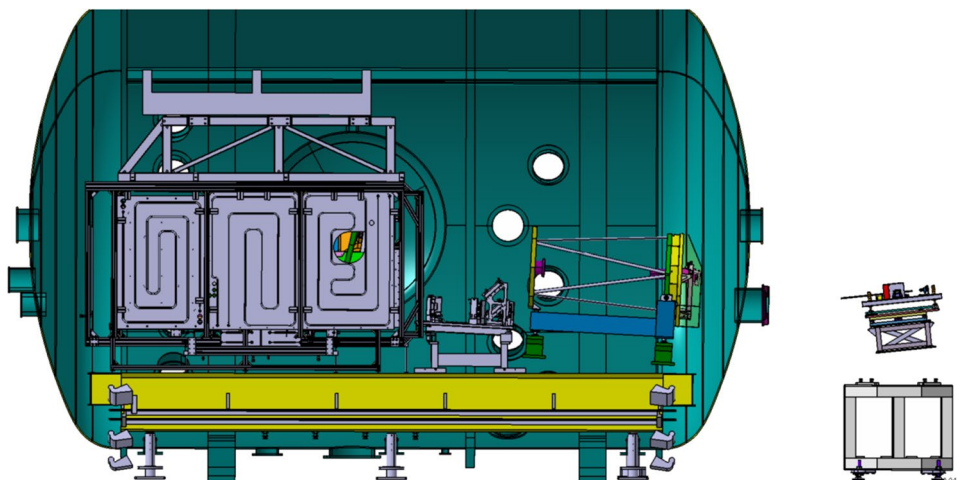
After closing the ATLID PFM, instrument verification will start with the ambient test campaign. This is aimed at characterizing the ATLID performance in ambient conditions. Several performance characteristics can be verified at this stage, being independent from environment, and it will be the first occasion to correlate the performance model and ensure consolidation of the estimated end to end performance. Ambient testing also includes electrical testing of the ATLID thermal components, followed by validation of the ACDM thermal functions.

Fig. 12 LCS integration on ATLID HSA

Fig. 13 Transport of SSA to inside of HSA (left) and SSA finally integrated on HSA (right)

Fig. 14 Integration of LCS evaporators on PLH's back wall, with ATLID pointing downwards

Last, the co-alignment control loop system will be operated in closed mode during ambient testing, thanks to OGSE returning attenuated emitted signal into the receiver part, at the level of and simulating atmospheric backscattering signal, with proper adjustment of ACDM timings. A perturbation on the return signal line of sight will test the loop actuation and characterize its corrective reaction. It will be a full system validation including the receiver co-alignment sensor (CAS), the Beam Steering Actuator (BSA) in the transmitter and the software module of the ACDM.

5 Pfm environmental test campaign overview

5.1 ATLID PFM vibration test

The Finite Element Model (FEM) has been refined with the objective to assess any need for input notch instruction. The PFM vibration test sequence is then similar to the one applied at OFM level, including monitoring of optical chain stability. Even if the most critical parts have been already tested, the PFM test remains the final validation of the whole assembled instrument and the verification of the assumptions made for the impact of the LCS at instrument level. Indeed, due to its specific design, the stiffness of its interface has a strong influence on the LCS dynamic behaviour. Its junction between two major and independent primary structures, i.e. on one hand the PLHs of the SSA (from OFM) and on the other hand the HSA (supporting EFM), increases consistently its mechanical specificity and complexity.

The knowledge of both structure behaviours, OFM & HSA, already tested separately under dynamic loads, gives good confidence on the FEM prediction. During the PFM test campaign, the various components of ATLID will be subjected to a range of acceleration varying from 10 to 120 g, (depending on their location on the structure). In this frame, the 1st ATLID mode on an infinitely stiff interface is above 60 Hz (i.e. OFM lateral mode Y 61.3 Hz coupled in ATLID structure).

5.2 ATLID PFM thermal vacuum test

The ATLID PFM thermal vacuum test will be performed in Centre Spatial de Liège facilities (CSL), in the Focal 5 chamber, as represented on Fig. 15. The instrument will be placed in the vacuum chamber inside a thermal tent to simulate the thermal space conditions. Inside the vacuum

Fig. 15 ATLID thermal vacuum test set-up, with ATLID inside Focal 5 chamber and OGSE focal plane outside the chamber

chamber the Optical Ground Support Equipment (OGSE) includes a large collimator with 70 cm aperture, to cover the receiver telescope, and a periscope that collects the emitted pulse to monitor energy level and to reinject it in the receiver side. Outside the vacuum chamber is a multipurpose OGSE focal plane with monitoring of energy and far field, with polarisation and line of sight control. The OGSE laser source is fibre injected into this focal plane.

The test sequence consists of the following activities:

- Instrument bake-out, with temperature limited at ATLID level to 50 °C due to sensitive units such as E-BEX;
- Non-Operational Phase, with representative environment temperatures, including a Thermal Balance for thermal model correlation purpose, and verification of the safe mode thermal hardware and thermal design;
- Operating Phases for the instrument nominal and redundant configurations, including a hot and a cold Thermal Balance in operating mode, performance tests in hot and cold conditions, thermal cycling and orbital cycling with representative environment temperatures.

Due to the orbit definition at 393 km and Mean Local Solar Time 13:45–14:00, the $+Y$ side of ATLID is submitted to variable sun fluxes, while the $-Y$ side of ATLID is not exposed to sun. During ATLID TV (thermal vacuum) test, the operating orbital cycling consists of fluctuations of the $+Y$ shroud in front of the Telescope radiator from -85 to $+15$ °C typically, while variations on the $-Y$ side are typically limited to 20 °C in amplitude.

Since the ATLID instrument is sensitive to Laser Induced Contamination (LIC) effects, particular precautions shall need to be taken during the ATLID TV campaign. All used materials are LIC compatible, and will be submitted to bake-out during the ATLID TV preparation, and several cold traps will be installed in the chamber. The emission path, being the most LIC-critical, will also be protected by an extension tube closed by a dedicated OGSE window, attached to the emission channel baffles. With such design any LIC effect, should it happen, will only impact the OGSE window, and not the flight EBEX window, that is the last and only optic being exposed to vacuum in orbit. The transmission will also be continuously monitored during the TV, at several places, and compared to the PLH internal emission energy sensor, which will allow observing and characterizing any transmission losses due to potential LIC effects on OGSEs.

6 Conclusion

After the development, qualification and delivery of all units, ATLID is now on its final steps of integration and approaching the start, as a self-standing and complete instrument,

of the performance tests in ambient. The model development philosophy, with parallel integration of the Optical Flight Model (OFM) and Electrical Flight Model (EFM), allowed the early verification of interfaces, performances and functional aspects, promoting the correction of operational aspects of the instrument and the improvement of OGSE's and test equipment. For that reason, these precursor activities are expected to have had a crucial positive impact on the success and efficient execution of the remaining test campaigns at instrument level. The test results obtained up to now are also very promising as concerns the performance aspects, suggesting a high probability of fulfilling ATLID specifications and consequently being fully in line with EarthCARE mission objectives.

With the execution of the environmental test campaign by end 2019, ATLID is expected to be then delivered for integration on the spacecraft platform and be subject to the satellite level test campaign, ultimately leading to the launch of the EarthCARE satellite.

References

1. EarthCARE: http://www.esa.int/esaLP/LPearthcare.html. Accessed May 2019
2. http://esamultimedia.esa.int/docs/SP_1279_1_EarthCARE.pdf. Accessed Apr 2004
3. Lefebvre, A., et al.: EarthCARE mission, overview, implementation approach and development status. In: Proceedings of SPIE 9881 (2016)
4. Hélière, A., et al.: Earth cloud, aerosol and radiation explorer optical payload development status. In: Proceedings of SPIE 10423 (2017)
5. Aida, Y., et al.: EarthCARE/CPR design results and PFM performance. In: Proceedings of SPIE 8889 (2013)
6. Wallace, K, et al.: Status of EC passive instruments payload. In: Proceedings of SPIE 9972 (2016)
7. Hélière, A., et al.: Development status of the EarthCARE Mission and its atmospheric Lidar. In: Proceedings of SPIE 9972-42 (2016)
8. Lefebvre, A., et al.: EarthCARE mission: approaching launch. In: IEEE International Geoscience and Remote Sensing Symposium (IGARSS) (2018)
9. de Villele, G., et al.: ATLID, ESA Atmospheric LIDAR: integration of instrument and tests. In: International Conference on Space Optics (ICSO) (2018)
10. ADM-AEOLUS, https://www.esa.int/Our_Activities/Observing_the_Earth/Aeolus/Introducing_Aeolus. Accessed May 2019
11. Pereira do Carmo, J., et al.: ATLID, ESA atmospheric lidar: manufacture and test results of instrument units. In: International Conference on Space Optics (ICSO) (2016)